Title: Using the quantum yields of photosystem II and the rate of net photosynthesis to monitor high irradiance and temperature stress in chrysanthemum (Dendranthema grandiflora)

Authors: Wakjera, E. J., Körner, O., Rosenqvist, E., & Ottosen, C.-O.

Article citation: Wakjera, E. J., Körner, O., Rosenqvist, E., & Ottosen, C.-O. (2015). Using the quantum yields of photosystem II and the rate of net photosynthesis to monitor high irradiance and temperature stress in chrysanthemum (Dendranthema grandiflora). *Plant physiology and biochemistry (Paris), 90*, 14-22. doi: http://dx.doi.org/10.1016/j.plaphy.2015.02.019

Using the quantum yields of photosystem II and the rate of net photosynthesis to monitor high irradiance and temperature stress in Chrysanthemum (*Dendranthema grandiflora*)

Eshetu Janka [a,*], Oliver Körner[b], Eva Rosenqvist[c], Carl-Otto Ottosen[d]

[a]Departement of Energy and Enviornmental Technology, Telemark University College, Kjølnes ring 56, 3918 Porsgrunn, Norway

[b]AgroTech A/S, Institute for Agri Technology and Food Innovation, Højbakkegård Allé 21, DK-2630 Taastrup, Denmark

[c]Department of Plant and Environmental Sciences, Crop Science, Copenhagen University, Højbakkegård Allé 9, DK-2630 Taastrup, Denmark

[d]Department of Food Science, Aarhus University, Kirstinebjergvej 10, DK- 5792 Årslev, Denmark

*Corresponding author. Tel.: +4741509113

E-mail address: eshetu.j.wakjera@hit.no

Abstract

Under a dynamic greenhouse climate control regime, temperature is adjusted to optimise plant physiological responses to prevailing irradiance levels; thus, both temperature and irradiance are used by the plant to maximise the rate of photosynthesis, assuming other factors are not limiting. The control regime may be optimised by monitoring plant responses, and may be promptly adjusted when plant performance is affected by extreme microclimatic conditions, such as high irradiance or temperature. To determine the stress indicators of plants based on their physiological responses, net photosynthesis (P_n) and four chlorophyll-*a* fluorescence parameters: maximum photochemical efficiency of PSII [F_v/F_m], electron transport rate [ETR], PSII operating efficiency [F'_q/F'_m], and non-photochemical quenching [NPQ] were assessed for potted chrysanthemum (*Dendranthema grandiflora* Tzvelev) 'Coral Charm' under different temperature (20, 24, 28, 32, 36 °C) and daily light integrals (DLI; 11, 20, 31, and 43 mol m^{-2} created by a PAR of 171, 311, 485 and 667 µmol m^{-2} s^{-1} for 16 h). High irradiance (667 µmol m^{-2} s^{-1}) combined with high temperature (>32 °C) significantly ($p < 0.05$) decreased F_v/F_m. Under high irradiance, the maximum P_n and ETR were reached at 24 °C. Increased irradiance decreased the PSII operating efficiency and increased NPQ, while both high irradiance and temperature had a significant effect on the PSII operating efficiency at temperatures >28 °C. Under high irradiance and temperature, changes in the NPQ determined the PSII operating efficiency, with no major change in the fraction of open PSII centres (q_L) (indicating a Q_A redox state). We conclude that 1) chrysanthemum plants cope with excess irradiance by non-radiative dissipation or a reversible stress response, with the effect on the P_n and quantum yield of PSII remaining low until the temperature reaches 28 °C and 2) the integration of online measurements to monitor photosynthesis and PSII operating efficiency may be used to optimise dynamic greenhouse control regimes and to detect plant stress caused by extreme microclimatic conditions.

Key words: chlorophyll-*a* fluorescence, dynamic greenhouse, extreme microclimate, stress detection, Q_A redox state

Abbreviations: C_i, inter cellular CO_2; DLI, daylight integral; ETR, electron transport rate; F_o, minimal fluorescence from dark-adapted leaf; F', fluorescence emission from light adapted leaf; F'_o, minimal fluorescence from light adapted leaf; F_m, maximal fluorescence from dark adapted leaf; F'_m, maximal fluorescence from light adapted leaf; F'_v, variable fluorescence from light adapted leaf; F'_q, difference in fluorescence between F'_m and F'; F_v/F_m, maximum photochemical efficiency of PSII; g_s, stomatal conductance; P_n, Net photosynthesis; PSII, photosystem II; NPQ, non-photochemical quenching; F'_q/F'_m, PSII operating efficiency ; Φ_{PSII}, the quantum efficiency of PSII; Φ_{NPQ}, the yield for dissipation by down-regulation; Φ_{NO}, the yield of other non-photochemical losses; q_L, fraction of PSII centres that are open; Q_A, (primary electron acceptor quinine); RH, relative humidity; VPD, vapour pressure deficit.

1. Introduction

A dynamic greenhouse climate control regime is based on plant physiology, outside solar irradiance and the microclimate of the crop within the greenhouse [1– 3]. Dynamic climate conditions facilitate greater precision in the regulation of temperature and humidity inside the greenhouse, thereby improving energy efficiency by reducing unnecessary heating or ventilation [2, 4, 5]. The temperature fluctuates more with solar irradiance under a dynamic control system compared to a traditional control system. This phenomenon allows the plants to utilise both temperature and irradiance to maximise the rate of photosynthesis, provided CO_2 is not limiting. The system optimises carbon gain at high irradiance, and reduces energy consumption at low irradiance [1, 6].

On sunny days, a dynamic greenhouse climate regime in a regular greenhouse may be compared to a semi-closed greenhouse type, because greenhouse air temperature is high due to a higher temperature set point and delayed screen folding, while vent opening is minimised via a higher ventilation set point. In addition, on a sunny day, plants may absorb more irradiance than needed for photosynthesis [7, 8]. With increasing greenhouse air temperature, plant tissue temperature may increase rapidly (i.e. within seconds; [9], due to low stomatal conductance, because stomata respond comparatively slowly (i.e. within minutes; [10]). This phenomenon may create both temporary and long-term stress reactions in the plants. Photosynthesis has a temperature optimum, depending on the irradiance, the growth temperature, CO_2 concentration and plant species [11, 12]. When the temperature rises above optimum, photosynthesis declines, at first gradually and reversibly, but, at a certain critical temperature level, the photosynthesis apparatus may be irreversibly damaged [13–15]. In most plants species, the light-saturated rates of photosynthesis decline as a direct response to extremely high temperatures, and operate at an optimum at intermediate temperatures [16].

Photoinhibition is one of the basic responses when plants are subjected to excess irradiance, representing the photo-inactivation of the photosynthetic apparatus [7, 17, 18]. Most plants have developed tolerance and/or acclimation mechanisms to avoid excess irradiance by different physiological mechanisms [19– 21]. For instance, an increase in non-radiative dissipation (NPQ: non-photochemical quenching of chlorophyll fluorescence) is a feedback regulatory mechanism induced upon exposure to high irradiance exceeding that which may be used at maximum quantum yield by photosystem II (PSII) [20, 22–26]. Previous studies have shown that low irradiance protects the photosynthetic apparatus from the adverse effects of high temperature, while photoinhibition protects against both high irradiance and high temperature stress [7, 27, 28]. Moreover, photoinhibitory and photooxidative damage to the photosynthetic apparatus represent plant responses to high irradiance and high temperature stress [17, 18, 29].

However, to advance the dynamic climate control regime based on photosynthesis, it is vital to understand plant responses under dynamic and potentially extreme greenhouse microclimate conditions. Therefore, in this study, we aimed to determine the stress indicators of plants based on their physiological responses by testing two hypotheses. First, it was hypothesised that an optimum physiological response may be provided for the early adjustment of a climate control system, especially when plant performance is affected by extreme microclimate conditions, such as excess light and high temperature. Second, it was hypothesised that integrating online measurements of physiological processes may assist climate control decisions under a dynamic climate control regime. Both high light and high temperature conditions were applied in a growth chamber, while both chlorophyll fluorescence and gas exchange were continuously measured under high light and temperature conditions in a greenhouse. The results of this study are anticipated to contribute towards enhancing dynamic climate control regime based on photosynthesis to maximise plant growth and, hence, the economic benefits of crop production.

2. Materials and Methods

2.1 Plant material

Cuttings of chrysanthemum were rooted in plastic pots (9.7 cm high, 11 cm diameter) and filled with a commercial peat mixed containing granulated clay (Pindstrup 2, Pindstrup A/S, Ryomgaard, Denmark) in a greenhouse at Aarhus University (Aarslev, Denmark 55° 22' N) in three different batches: (1) spring (06/04–30/04/2012); (2) spring/summer (30/04–16/06/2012); and (3) summer/fall (10/08–10/09/2012).

The plants were grown on a growing bench in the greenhouse at a plant density of 40 plants per m^2. The greenhouse climate data for the three batches is in Table 1. Nutrients (macronutrients: N, 185 ppm; P, 27 ppm; K, 171 ppm; and Mg, 20 ppm; micronutrients: Ca, Na, Cl, 18 ppm; SO_4, 27 ppm; Fe, 0.9 ppm; Mn, 1.17 ppm; B, 0.25 ppm; Cu, 0.1ppm; Zn, 0.77 ppm; and Mo, 0.05 ppm) were incorporated into the irrigation water, and automatically supplied twice a day as ebb and flood irrigation (08:45 and 16:15). The electrical conductivity (EC) of the irrigation water was 1.88 µS cm^{-1} and the pH was 5.8. Biological controls against insects were used twice during the growing period.

2.2 Temperature and irradiance treatments

The first two experiments were conducted in a growth chamber (MB-teknik, Brøndby, Denmark). The two experiments included two combinations of three different temperatures (Experiment 1: 20, 24 and 28 °C; Experiment 2: 20, 32 and 36 °C; Table 2). In each experiment, a total of 240 six week old uniformly sized plants (plant height of 0.12 ± 0.01 m) were transferred from the greenhouse to three growth chambers. For the higher temperature settings (28, 32 and 36 °C), the temperature was increased stepwise (1–2 °C every 2 h) in the climate chamber on the first day, to avoid temperature shock.

In each growth chamber, four irradiance levels were created by combining shading screens with different transmissions (F-80 Extra, Fibertex Nonwovens A/S, Aalborg, Denmark and P19 Utrasil, Lundhede Planteskole, Feldborg, Denmark). Three rectangular aluminium frames (width x length x height = 0.78 x 1.13 x 0.83 m) were constructed for each chamber, and the frames were covered with the screen material, which covered two-thirds of the frame height from the top, to ensure that the minimum irradiance was reflected from the side, in addition to supplying sufficient air movement under the screens. The frames were placed above the bench, leaving an open space for full light. The irradiance in the open space and inside each frame with the screens was measured at pot height (0.11 m), 0.25 m and 0.35 m high (maximum plant height) above the bench using a quantum sensor (LI-250 Irradiance meter, LI-COR, Lincoln, Nebraska, USA). At each level of irradiance, 20 plants were used, with a total of 80 plants per chamber. The treatments were a factorial combination of five temperatures and four light levels.

The light source was metal halide lamps (HQI, 400W, Osram, Munich, Germany), operated at a 16 h/8 h light/dark photoperiod. The CO_2 level in the chambers was maintained at 600 µmol mol^{-1}. The vapour pressure deficit (VPD) was kept constant at 0.82 (± 0.004) kPa for each temperature using different relative humidity levels (Table 2). Irradiance (LI-190SA quantum sensor, Lincoln, USA), air temperature (Pt 100 DIN 43760B, Helsinki, Finland) and air humidity (Humitter 50U, Helsinki, Finland) were recorded at 5-min intervals with a data logger (dataTaker DT605, CAS DataLoggers, Chillicothe OH, USA).

2.3 Chlorophyll-a fluorescence measurement

Chlorophyll-*a* fluorescence was measured before the plants were transferred to the growth chambers and during the treatment period when it was placed alternately in each batch for three days. The measurement was done in the morning (2 h after the light was switched on) and in the afternoon (3 h before the light was switched off) using a plant efficiency analyser (PEA) (Hansatech

Instruments, Kings Lynn, UK) after dark-adapting the leaves for 30 min using a leaf clip (Hansatech, Instruments, Kings Lynn, UK), and then subsequently exposing the leaves to 3000 µmol m^{-2} s^{-1} measuring irradiance to generate maximal fluorescence (F_m) [30–33], to measure the maximum photochemical efficiency $F_v/F_m = (F_m - F_o)/F_m$ of dark adapted leaves. In parallel, a MINI-PAM (Walz, Effeltrich, Germany) was used to measure the PSII operating efficiency $F'_q/F'_m = (F'_m - F')/F'_m$ [34] and linear electron transport rate (ETR), which were calculated as described by Genty et al. [35], at the ambient irradiance in the treatments.

2.4 Gas exchange measurement

Net photosynthesis (P_n) and stomatal conductance (g_s) were measured on three randomly selected plants from each treatment on the third or fourth fully developed and illuminated leaves for three subsequent days during the treatment period. The IRGA system (CIRAS-2, PP-systems, MA, USA) was used for this measurement. The irradiance, temperature and relative humidity of the leaf cuvette was set according to treatment, and recorded when P_n was at a steady state.

2.5 Long term measurements of fluorescence

Diurnal changes and acclimation (e.g. short or long term) of PSII was monitored for the same leaf in each treatment. One measuring head (compact/robust metal tube of 3 cm diameter and 22 cm length with a complete PAM chlorophyll fluorometer) was used per light treatment and a total of four measuring heads were used in the Monitoring-PAM (Walz, Eifeltrich, Germany), which were connected to a Moni-Bus (Field bus, RS485) and computer controlled by the WinControl-3 software (Version 2.xx). The Moni-PAM continuously measured the fluorescence emission from the light adapted leaf (F'), the maximum fluorescence during saturating pulses (F'_m), irradiance and leaf temperature were measured every 30 min, from which the PSII operating efficiency was calculated, F'_q/F'_m. The mean measurements of F'_m at night was used as maximal fluorescence from dark adapted leaves (F_m), and was used to calculate the fraction of open PSII based on the lake

model for the photosynthetic unit (q_L) and heat dissipation through non-photochemical quenching (NPQ) [32]. Furthermore, in addition to the PSII operating efficiency (F'_q/F'_m), which, in the nomenclature of Kramer et al. [36], is the quantum efficiency of PSII, Φ_{II}, the quantum yield of the down-regulatory non-photochemical process (Φ_{NPQ}) and the quantum yield for other energy losses (Φ_{NO}) were also calculated, where $\Phi_{II} + \Phi_{NPQ} + \Phi_{NO} = 1$ [36] (Table 3).

The Moni-PAM was also used to obtain long-term measurements in the greenhouse on sunny days, where the average daily irradiance integral exceeded 12 mol m^{-2} day^{-1}. Microclimate data, such as air temperature, leaf temperature and humidity, were measured using the methods described in Section 2.2.

2.6 Data analysis

To avoid the outlier effect, a function *mvoutlier* (R-package, version 2.15.0) was applied to identify any outliers. A univariate normality test was applied to test the normality, and the Bartlett test function was used to test the equality of variance of the data. The means of the F_v/F_m, F'_q/F'_m, q_L, NPQ and P_n were used for analysis of variance (ANOVA). The experimental design was a split plot, where temperature was the main factor and irradiance was the split factor. A nonlinear mixed effect model for repeated measurement was used to test interactions between factors. Treatment effects were tested at the 5% probability level. R version 2.15.0 (www.r-project.org) was used for ANOVA and regression analysis, while SigmaPlot 11.0 (Systa software, Inc. Washington USA) was used for graphics.

3. Results

3.1 Maximum photochemical efficiency of PSII (F_v/F_m) and the electron transport rate (ETR)

The statistical analysis showed that irradiance and temperature had a significant interaction effect on F_v/F_m by the third day of the treatment ($P < 0.05$). At a low temperature (20 °C) F_v/F_m was 4% lower at high irradiance compared to low irradiance; however, this value changed to 12% when the temperature was high (36 °C) (Fig. 1A). The decrease in F_v/F_m was highly correlated with increased irradiance and temperature. For instance, an increase in irradiance from 171 to 667 µmol m^{-2} s^{-1} decreased F_v/F_m by 4 to 10% at the high temperature of 36 °C. The effect of irradiance was consistent during the treatment period and, on day six of the treatment, the irradiance and temperature showed significant interaction ($P < 0.01$) effect on F_v/F_m. However, after day five, the difference in F_v/F_m between the irradiance levels (high and low) at each temperature setting reduced until the temperature exceeded 32 °C, while the effect of high irradiance and high temperature showed a significant decline of F_v/F_m at 36 °C (Fig. 1B).

Irradiance and temperature had a significant interaction effect on the ETR on the third and sixth day of the treatment (Fig. 1C, D). The ETR was high at 20 °C and 24 °C under high light conditions, exhibiting the most pronounced temperature optimum at 24 °C under high light conditions on the sixth day of the treatment. However, at lower irradiances, there was no significant change in ETR with increasing temperature. At the two high light levels, ETR overlapped at temperatures ≥28 °C, indicating that light saturation had already been reached at around 485 µmol m^{-2} s^{-1} under these conditions.

3.2 Gas exchange (P_n) and stomatal conductance (g_s)

The photosynthesis measured at the ambient irradiance showed that P_n was significantly different ($P < 0.01$) for the irradiance levels under the respective temperature treatments, with the temperature optimum being 24 °C for all irradiance levels (Fig. 2A). The P_n slowly declined above

the temperature optimum and the difference between the irradiance levels decreased with increasing temperature above the temperature optimum. There was no significant difference in P_n among the temperatures at the low irradiance level (171 µmol m^{-2} s^{-1}). The g_s showed no significant difference for the various irradiance and temperature combinations, except at 24 °C, where g_s was high at the two lowest irradiances (Fig. 2B). The same pattern was observed for the measurement of intercellular CO_2 (C_i) (Fig. 2C).

3.3 PSII operating efficiency (F'_q/F'_m), fraction of open PSII (q_L) and non-photochemical quenching (NPQ) (long term measurements of fluorescence)

Monitoring F'_q/F'_m, q_L and NPQ in the controlled climates based on dark-adapted F_m values from the previous night showed that irradiance had a significant effect ($P < 0.01$), in addition to a clear interactive effect of irradiance and temperature (Fig. 3). F'_q/F'_m decreased with increasing irradiance, with the rate of decrease being dependent on temperature. At 24 °C, the decrease in F'_q/F'_m stopped at 485 µmol m^{-2} s^{-1} (Fig. 3A), whereas it continued to decrease to 667 µmol m^{-2} s^{-1} at 32 °C (Fig. 3B). q_L primarily decreased to 485 µmol m^{-2} s^{-1}, and was generally unaffected by temperature (Fig. 3B, E). At the two lowest irradiances, NPQ was not affected by temperature; however, at the two highest irradiances, NPQ increased with increasing temperature, exhibiting more fluctuations through the day as irradiance increased (Fig. 3C, F).

3.4 The quantum yield of the competing pathways for de-excitation; ΦPSII, Φ_{NPQ} and Φ_{NO} (long term measurements of fluorescence)

The Moni-PAM measurements were used to calculate the quantum yield of the competing pathways for de-excitation based on the equations of Kramer et al. (2004) (Fig. 4). The quantum efficiency of photosystem II (Φ_{PSII}, = F'_q/F'_m, is PSII operating efficiency based on Baker and Rosenqvist 2004) decreased with increasing irradiance, but was not affected by temperature (Fig. 4A–C), except under the highest irradiance (32 °C and 36 °C), where it decreased (Fig. 4D). This

effect was balanced by a slight increase in both Φ_{NPQ} and Φ_{NO} with increasing light (Fig. 4A–C), except under the highest irradiance (32 °C and 36 °C), where Φ_{NPQ} increased in a similar pattern to Φ_{PSII} (Fig. 4D).

The continuous measurement of F'_q/F'_m in the greenhouse showed a direct relationship with irradiance and leaf temperature during the course of the day, where a significant decrease was observed during the middle of the day with an increase in irradiance and leaf temperature (Fig. 5). F'_q/F'_m and NPQ were more dynamic with fluctuating irradiance conditions in the greenhouse. The NPQ showed an increase with increasing irradiance and leaf temperature, which resulted in a decrease in F'_q/F'_m (Fig. 5D), while q_L never dropped below 0.5, indicating that PSII was ≥50% open at all times (Fig. 5E).

4. Discussion

4.1 Maximum photochemical efficiency of PSII (F_v/F_m), electron transport rate (ETR) and gas exchange (P_n)

The current study demonstrated that the combination of high irradiance and high temperature caused the photoinhibition (i.e. decrease in F_v/F_m; [28] of chrysanthemum. Specifically, the highest level of irradiance had a significant negative effect on F_v/F_m at high temperatures. Furthermore, as irradiance increased, F_v/F_m decreased at each temperature, with temperature having a limited effect during the first three days of the treatment (Fig. 1A). The short term stress that caused the F_v/F_m to decrease at higher irradiances was attributed to partial photoinhibition [37, 38]. The F_v/F_m slightly increased after the third day of the treatment, except under temperature conditions exceeding 32 °C, with F_v/F_m significantly declining under high irradiance (Fig. 1B). This result shows that, during the final days of the treatment, acclimation to high irradiance might have alleviated the effect of high irradiance on F_v/F_m at temperatures below 32 °C. In contrast, at temperatures above 32 °C, temperature mediated photoinhibition might have been occurred [39, 40]. In general, the decrease in

F_v/F_m occurs as a result of the inactivation of PSII photochemistry and/or the increase in thermal energy dissipation from PSII associated chlorophyll antennae [28]. The acclimation of photosynthesis to high irradiance may arise due to an increase in PSII and a concomitant decrease in light harvesting complex II (LHCII); in other words, reduced antenna size is matched by a corresponding increase in the number of PSII units [41].

The acclimation of F_v/F_m over time for plants under high irradiance and low temperature (below 28 °C) conditions possibly indicates that the PSII is protected by a mechanism that dissipates excess energy (NPQ) to prevent the photosynthetic apparatus from becoming damaged. Plants grown under high irradiance often have substantially increased capacities for ΔpH-dependent protective energy dissipation [41]. However, when high irradiance was combined with high temperature in the current experiment, the F_v/F_m decreased significantly. This phenomenon might be associated with the effect of high temperature on the PSII reaction centre [30, 42, 43]. The current study indicated that the PSII reaction centre might be damaged by temperatures above 28 °C combined with high irradiance. Even though it is extremely important to dissipate excess irradiance to avoid possible photo-damage to the PSII, the current study demonstrated that this response would cause a major reduction in the net gain of CO_2 when temperature stress was imposed under high irradiance conditions (Fig. 2A).

At all irradiance levels, ETR and P_n reached an optimum at 24 °C (Fig. 1C, D, Fig. 2A), whereas ETR noticeably changed above 28 °C under high irradiance conditions. Hence, this study demonstrates that ETR, g_s and C_i limitation (Fig. 2B and C) do not cause a decline in P_n with increasing temperature (Fig. 2B and C). Rather, we found that this phenomenon is caused by to photorespiration (i.e. embraces several processes associated with O_2 uptake in the light, photoinhibition and photorespiration [44]), supporting previous studies [44–46]. Moreover, reversible photoinhibition of PSII efficiency is prevalent under high irradiance conditions and hence

non-stomatal factors play a major role in regulation photosynthesises under high irradiance and high temperature stress [46]. A decrease in PSII operating efficiency is always accompanied by an increase in NPQ [24, 47], as a reversible down regulation of PSII under high irradiance conditions [18, 48]. As Chrysanthemum are able to cope with excess irradiance at temperatures below 28 °C, we suggest that the process involved in acclimating the photosynthetic apparatus to high irradiance and temperature stress might be due to changes in the efficiency of the open PSII reaction centre and the dissipation of excess absorbed energy (NPQ) [48, 49].

4.2 PSII operating efficiency (F'_q/F'_m), fraction of open PSII centres (q_L) and non-photochemical quenching (NPQ)

F'_q/F'_m is determined by the concentration of open PSII reaction centres and the efficiency of excitation energy capture by the open PSII centres [35]. However, in the current study, F'_q/F'_m declined under high irradiance and high temperature conditions (Fig. 3D), because temperature stress enhances the extent of photoinhibition [27, 50]. The decrease in F'_q/F'_m was accompanied by a decrease in q_L, which is an indicator of the Q_A redox state [36]. However, as more than 50% of PSII centres were open (Fig. 3B, E) we concluded that the PSII operating efficiency was primarily determined by changes in NPQ (Fig. 3C, F). Furthermore, Kramer *et al*. [36] showed that a large increase in NPQ induces a large decrease in PSII operating efficiency, with little change in q_L.

4.3 The quantum efficiency of PSII (Φ_{PSII}), yield for dissipation by down-regulation (Φ_{NPQ}) and yield of other non-photochemical losses (Φ_{NO})

The exciton fraction dissipated via photochemistry (Φ_{PSII}) and via the two competing non-productive pathways (Φ_{NPQ} and Φ_{NO}) [36], based on estimates for the different temperature and light combinations (Fig. 4). Our data showed that high temperature (i.e. above 28 °C) combined with high irradiance increased the extent of PSII photoinactivation through increased Φ_{NPQ} and decreased Φ_{PSII}. It has been previously shown that PSII photoinactivation is indirectly dependent on

the level of thermal energy dissipation [23, 47]. Supporting previous studies, the current study demonstrated that Φ_{NO} was relatively stable for all temperature and light combinations, as a result of compensatory changes in Φ_{PSII} and Φ_{NPQ} [36]. We suggest that high irradiance and temperature above 28 °C might limit the capacity of NPQ to regulate light capture by Chrysanthemum. In comparison, certain stress tolerant plant species are able to cope with high irradiance and high temperature by an effective regulating mechanism in energy partitioning of PSII complexes [49].

Under greenhouse conditions, Chrysanthemum plants tend to respond to high irradiance and high leaf temperature (Fig. 5A, B) by decreasing the PSII operating efficiency and increasing the NPQ, but with minimal change in q_L (Fig. 5C–E). The increase in leaf temperature might be associated with the possible closure of stomata at midday [51]. Therefore, by down-regulating the PSII operating efficiency through increasing NPQ might cause an increase in photorespiration when CO_2 is a limiting factor. Moreover, under high irradiance, increased capacities for NPQ and photorespiration are essential to avoid photoinhibitory damage and to tolerate high temperature stress under excess irradiance [44].

5. Conclusions

A dynamic climate control regime facilitates the precise regulation of high temperature and irradiance conditions, under which a plant may utilise both temperature and irradiance to maximise the rate of photosynthesis. However, we also observed that excess irradiance and high temperature (above 28 °C) creates temperature mediated photoinhibition and photorespiration, which may cause temporary or long-term stress on Chrysanthemum plants. Yet, the effect of photorespiration may be alleviated by elevating CO_2 concentrations, which is a regular practice in greenhouse cultivation. Therefore, the continuous monitoring of plant responses, based on the quantum yields of PSII and photosynthetic rates, provides a useful tool for predicting both short- and long-term stress resulting from extreme microclimate conditions. In conclusion, continuous monitoring systems could be up-

scaled from the leaf- to the crop-level, with crop models being used to assist with real-time stress detection.

Acknowledgements

This research was part of the project *itGrows* funded by The Danish High Technology Foundation. Additional funding was provided by the European Regional Development Fund (ERDF) and EU project "GreenGrowing".

References

[1] J.M. Aaslyng, N. Ehler, P. Karlsen, E. Rosenqvist, IntelliGrow: A component based climate control system for decreasing the greenhouse energy consumption, Acta Hortic. 507 (1999) 35–41.

[2] J.M. Aaslyng, J.B. Lund, N. Ehler, E. Rosenqvist, IntelliGrow: a greenhouse component-based climate control system, Env.Mod. & Software. 18 (2003) 657–666.

[3] O. Körner, J.M. Aaslyng, A.U. Andreassen, Microclimate prediction for dynamic greenhouse climate control, Hortscience 42 (2007) 272–79.

[4] O. Körner, H. Challa, Temperature integration and process-based humidity control in chrysanthemum, Comput. Electron. Agr. 43 (2004) 1–21.

[5] O. Körner, G.Van Straten, Decision support for dynamic greenhouse climate control strategies, Comput. Electron. Agr. 60 (2008) 18–30.

[6] C.O. Ottosen, E. Rosenqvist, L. Sørensen, Effect of a dynamic climate control on energy saving, yield and shelf life of spring production of bell peppers (*Capsicum annumm L.*). Europ. J. Hort. Sci 68 (2003) 26–31.

[7] S.P.Long, S. Humphries, P.G. Falkowski, Photoinhibition of photosynthesis in nature. Annu. Rev. Plant Phys. 45 (1994) 633–62.

[8] C.Wilhelm, D. Selmar, Energy dissipation is an essential mechanism to sustain the viability of plants: The physiological limits of improved photosynthesis. J. Plant Physiol. 168 (2011) 79–87.

[9] H.G. Jones, Plants and Microclimate: A quantitative approach to environmental plant physiology University Press, Cambridge,1992.

[10] S. Chamont, D. Strainchamps, S. Thunot, Short- and long-term stomatal responses to fluctuations in environment in southern European greenhouses. Ann. Bot. London 75 (1995) 39–47

[11] J. Berry, O. Björkman, Photosynthetic response and adaptation to temperature in higher plants. Annu. Rev. Plant Physiol. 31 (1980) 491–43.

[12] O. Björkman, in: J. Grace, E.D. Ford, P.G. Jarvis (Eds.), Plants and Their Atmospheric Environment, Oxford Blackwell, Edinburgh, 1981, pp. 273–301.

[13] A. Melis, Photosystem-II damage and repair cycle in chloroplasts: what modulates the rate of photodamage in vivo? Trends Plant Sci. 4 (1999) 130–135.

[14] S. Takahashi, M.R. Murata, How do environmental stresses accelerate photoinhibition? Trends Plant Sci. 13 (2008) 178–82.

[15] S. Takahashi, M.R. Badger, Photoprotection in plants: a new light on photosystem II damage. Trends Plant Sci. 16 (2011) 53–60.

[16] K. Hikosaka, K. Ishikawa, A. Borjigidai, O. Muller, Y. Onoda, Temperature acclimation of photosynthesis: mechanisms involved in the changes in temperature dependence of photosynthetic rate. J. Exp. Bot. 291 (2006) 291–302.

[17] S.B. Powles, Photoinhibition of photosynthesis induced by visible light. Annu. Rev. Plant Physiol. 35 (1984) 15–44.

[18] E. Tyystjärvi, Photoinhibition of photosystem II. Int. Rev. Cell Mol. Biol. 300 (2013) 243–303.

[19] N.E. Holt, G.R. Fleming, K.K. Niyogi, Toward an unerstanding of the mechanism of the nonphotochemical quenching in green plants. Biochemistry 43 (2004) 8281–9.

[20] P. Horton, M. Wentworth, A. Ruban, Control of the irradiance harvesting function of chloroplast membranes: The LHCII-aggregation model for non-photochemical quenching. FEBS L 579 (2005) 4201–06.

[21] Z. Yanhong, H.M. Lam, J. Zhang, Inhibition of photosynthesis and energy dissipation induced by water and high light stresses in rice. J. Exp. Bot. 58 (2007) 1207–17.

[22] P. Horton, A. Ruban, R.G. Walters, Regulation of light harvesting in green plants. Annu. Rev. Plant Phys. 47 (1996) 655–84.

[23] K.K. Niyogi, Photoprotection revisited: Genetic and molecular approaches. Annu. Rev. Plant Phys. 50 (1999) 333–59.

[24] B. Demmig-Adams, W.W. Adams III, Photoprotection in an ecological context: the remarkable complexity of thermal energy dissipation. New Phytol. 172 (2006) 11–21.

[25] M. Brestic, M. Zivcak, K. Olsovska, S. Hong-Bo, M. H. Kalaji, I. S. Allakhverdiev, Reduced glutamine synthetase activity plays a role in control of photosynthetic responses to high light in barley leaves. Plant Physiol. Biochem. 81 (2014) 74-83.

[26] M. Zivcak, M. Brestic, M.H. Kalaji, Govindjee, Photosynthetic responses of sun and shade grown barley leaves to high light: Is the lower PSII connectivity in shade leaves associated with protection against excess of light? Photosynth. Res. 119 (2014) 339-354.

[27] N. Murata, S. Takahashi, Y. NIshiyama, S.I. Allakhverdiev, Photoinhibition of photosystem II under environmental stress. Biochim. Biophys. Acta 1767 (2007) 414–21.

[28] W.W. Adams III, O. Muller, C.M. Cohu, B. Demming-Adams, May photoinhibition be a consequence, rather than a cause of limited plant productivity. Photosynth. Res. 117 (2013) 31–44.

[29] I. Vass, Molecular mechanisms of photodamage in the photosystem II complex. Biochim. Biophys. Acta 1817 (2012) 209–17.

[30] S. Mathur, S.I. Allakhverdiev, A. Jajoo, Analysis of high temperature stress on the dynamics of antenna size and reducing side heterogeneity of Photosystem II in wheat leaves (*Triticum aestivum*). Biochim. Biophys. Acta 1807 (2011) 22–9.

[31] R.J. Strasser, A. Srivastava, M.M. Tsimilli, in: M. Yunus, U. Pathre, Mohanty (Eds), The fluorescence transient as a tool to characterize and screen photosynthetic samples, Probing Photosynthesis: Mechanism, regulation and adaptation. Taylor and Francis, London, 2000, pp 443–80.

[32] M.H. Kalaji, G. Schansker, R. J. Ladle, V. Goltsev, K. Bosa, S.I. Allakhverdiev, M. Brestic, F. Bussotti, A. Calatayud, P. Dąbrowski, N. I. Elsheery, L. Ferroni, L. Guidi, S.W. Hogewoning, A. Jajoo, A. N. Misra, S.G. Nebauer, S. Pancaldi, C. Penella, D.B. Poli, M. Pollastrini, Z.B. Romanowska-Duda, B.Rutkowska, J. Serôdi, K. Suresh, W. Szulc, E. Tambussi, M. Yanniccari, M. Zivcak, Frequently Asked Questions about in vivo chlorophyll fluorescence: practical issues. Photosynth Res 122 (2014) 121–158.

[33] M.H. Kalaji, V. Goltsev, K. Bosa, S.I. Allakverdiev, R.J. Strasser, Govindjee, Experimental in vivo measurements of light emission in plants: a perspective dedicated to David Walker. Photosynth Res 114 (2012) 69-96.

[34] N.R. Baker, E. Rosenqvist, Application of chlorophyll fluorescence can improve crop production strategies: an examination of future possibilities. J. Exp. Bot. 55 (2004) 1607–21.

[35] B. Genty, J.M. Briantais, N.R. Baker, The relationship between the quantum yield of photosynthetic electron transport and quenching of chlorophyll fluorescence. Biochim. Biophys. Acta 990 (1989) 87–92.

[36] D.M. Kramer, G. Johnson, O. Kiirats, G.E. Edwards, New fluorescence parametrs for the determination of Q_A rdox state and excitation energy fluxes. Photosynth. Res. 77 (2004) 209–18.

[37] E. Rosenqvist, G. Wingsle, E. Ögren, Photoinhibition of photosynthesis in intact willow leaves in response to moderate changes in irradiance and temperature. Physiol. Plant 83 (1991) 390–96.

[38] M.H. Kalaji, R.Carpentier, S.I. Allakhverdiev, K. Bosa, Fluorescence parameters as an early indicator of light stress in barley. J. Photochem. Photobiol. B: Biol. 112 (2012) 1-6.

[39] M. Štroch, D. Vráble, J. Podolinská, J. Kalina, O. Urban, V. Špunda, Acclimation of Norway photosynthetic apparatus to the combined effect of high irradiance and tempeature. J. Plant Physiol. 167 (2010) 597–605.

[40] D. Kornyeyev, S. Holaday, B. Logan, Predicting the extent of photosystem II photoinactivation using chlorophyll a fluorescence parameters measured during illumination. Plant Cell Physiol. 44 (2003) 1064–70.

[41] G.R. Walters, Towards an understanding of photosynthetic acclimation . J. Exp. Bot. 56 (2005) 435–47.

[42] E. Janka, O. Körner, E. Rosenqvist, C.O. Ottosen, High temperature stress monitoring and detection using chlorophyll a fluorescence and infrared thermography in chrysanthemum (*Dendranthema grandiflora*). Plant Physiol. Biochem. 67 (2013) 87–94.

[43] M.H. Kalaji, K. Bosa, J. Kościelniak, Z. Hossain, Chlorophyll a fluorescence - A useful tool for the early detection of temperature stress in spring barley (Hordeum vulgare L.). OMICS: A Journal of Integrative Biology 15 (2011) 925-934

[44] C.B. Osmond, S.C. Grace, Perspectives on photoinhibition and photorespiration in the field: quintessential inefficiencies of the light and dark reactions of photosynthesis. J. Exp. Bot. 46 (1995) 1351–1362.

[45] H. Muraoka, Y. Tang, I. Terashima, H. Koizumi, I. Washitani, Contributions of diffusional limitation, photoinhibition and photorespiration to midday depression of photosyntheis in *Arisaema heterophyllum* in natural high light. Plant Cell Environ. 23 (2000) 235–50.

[46] J.L. Jifon, J.P. Syvertsen, Moderate shade can increase net gas exchange and reduce photoinhibition in citrus leaves. Tree Physiol. 23 (2003) 119–127.

[47] B. Demmig-Adams, , W.W. Adams III, Photoprotection and other responses of plants to high light stress. Annu. Rev. Plant Phys. 43 (1992) 599–626.

[48] F.l.L Figueroa, C. Jiménez, L.M. Lubián, O. Montero, M. Lebert, DP. Häder, Effects of high light and temperature on photosynthesis and photoinhibition in *Nannochloropsis gaditana* Lubián (Eustigmatophyceae). J. Plant Physiol. 151 (1997) 6–15.

[49] L. Song, S.W. Chow, L. Sun, C. Li, C. Peng, Acclimation of phtosystem II to high temperature in two Wedelia species from different geographical origins: implications for biological invasions upon global warming. J. Exp. Bot. 61(14) (2010), 4087–96.

[50] X. Yang, X. Wen, H. Gong, Q. Lu, Z. Yang, Y. Tang, Z. Liang, C. Lu, Genetic engineering of the biosynthesis of glycinebetaine enhances thermotolerance of photosystem II in tobacco plants. Planta 225 (2007) 719–33.

[51] R. Zweifel, J.P. Böhm, R. Häsler, Midday stomatal closure in Norway spruce – reactions in the upper and lower crown. Tree Physiol. 22 (2002) 1125–36.

Table 1 The climate set point and measured climate data in the greenhouse for each experimental period. Climatic parameters were collected by respective climatic sensors at 10 min intervals, with the data being recorded on a climate computer. Values are means ± SE, n = 4.

Exp.	Date	Set points				Measured climatic parameters				
		Temp. (°C, day/night)	RH (%)	VPD (kPa)	CO_2 (µmol mol^{-1})	Temp. (°C, day/night)	RH (%)	VPD (kPa)	CO_2 (µmol mol^{-1})	DLI (mol m^{-2})
I	06/04–30/04 2012	24/18	60	0.82	600	24/21 (± 0.1)	48.0 (±0.2)	1.65 (±0.09)	587 (±4.9)	9.6
II	30/04–16/06 2012	24/24	60	0.82	600	26/26 (± 0.1)	45.8 (±0.2)	1.98 (±0.09)	461.2 (±3.8)	11.5
III	10/08–10/09 2012	20/20	60	0.82	600	24/24 (± 0.1)	50.7 (±0.2)	1.75 (±0.18)	536 (±5.7)	12.9

Table 2 The five irradiance and temperature treatment combinations in the growth chambers. Irradiance was measured at maximum plant height (n = 5). The VPD was set to a constant level by varying the RH. The CO_2 concentration was kept the same in all treatments.

Treatments	Temperature (°C, day/night)	DLI (mol m^{-2})	VPD (kPa)	RH (%)	CO_2 (µmol mol^{-1})
I	20/20	11 (± 1.03)	0.82	65	600
		20 (± 1.22)			
		31 (± 2.51)			
		43 (± 0.72)			
II	24/22	11 (± 1.03)	0.82	72	600
		20 (± 1.22)			
		31 (± 2.51)			
		43 (± 0.72)			
III	28/26	11 (± 1.03)	0.82	78	600
		20 (± 1.22)			
		31 (± 2.51)			
		43 (± 0.72)			
IV	32/30	11 (± 1.03)	0.82	83	600
		20 (± 1.22)			
		31 (± 2.51)			
		43 (± 0.72)			
V	36/34	11 (± 1.03)	0.82	86	600
		20 (± 1.22)			
		31 (± 2.51)			
		43 (± 0.72)			

Table 3 Chlorophyll fluorescence parameters used, descriptions of how they are used to analyse irradiance and their temperature effect on PSII, in addition to the equations used to calculate respective parameters.

Parameter	Description	Formula	Reference
F'_o	Minimum fluorescence from light adapted leaf	$F'_o = F_o/(F_v/F_m + F_o/F'_m)$	[34]
Φ_{PSII}/ F'_q/F'_m	Quantum efficiency or operating efficiency of PSII	$\Phi_{PSII} = F'_q/F'_m = F'_m - F'/ F'_m$	[34, 36]
ETR	Linear electron transport	$ETR = F'_q/F'_m * 0.5 * 0.84$	[35]
NPQ	Non-photochemical quenching	$NPQ = (F_m/F'_m) - 1$	[34]
Φ_{NPQ}	Yield for dissipation by down-regulation	$\Phi_{NPQ} = 1- F'_q/F'_m - 1/(NPQ + 1 + q_L*(F_m/F_o - 1)$	[36]
Φ_{NO}	Yield of other non-photochemical losses	$\Phi_{NO} = 1/(NPQ + 1 + q_L*(F_m/F_o - 1)$	[36]
q_L	Fraction of open PSII centres (lake model for PSU)	$q_L = (F'_q/F'_v)*(F'_o/F')$	[34]

Legends of figures

Fig. 1 The fluorescence parameters as a function of temperature at the four irradiance levels. The maximum photochemical efficiency (F_v/F_m) measured from a dark-adapted leaf for 30 min on the third (A) and sixth (B) day of the stress treatment. The electron transport rate (ETR) on the third (C) and sixth day (D) of the stress treatment. The standard was 20 °C with a PAR of 171 μmol m^{-2} s^{-1}. The error bar represents the standard error and n = 5.

Fig. 2 Net leaf photosynthesis (A), stomatal conductance (B) and inter cellular CO_2 as a function of temperature at the four irradiance levels on the sixth day of the stress treatment. The error bar represents the standard error and n = 5.

Fig. 3 The diurnal change of PSII operating efficiency, fraction of PSII centres that were open (q_L) and non-photochemical quenching (NPQ) at the four irradiance levels and at two temperatures, 24 °C (A, B and C) and 32 °C (D, E and F), respectively. Fluorescence parameters were measured every 30 min, and the data was averaged using 2.5 h intervals. The error bar represents the standard error and n = 5.

Fig. 4 Effects of temperature on the quantum efficiency of PSII (Φ_{PSII}), the yield for dissipation by down-regulation (Φ_{NPQ}) and the yield of other non-photochemical losses (Φ_{NO}) at the four irradiance levels. The error bar represents the standard error and n = 5.

Fig. 5 Irradiance on typical sunny days during August 2012 in a greenhouse (A), leaf temperature (B), the diurnal course of PSII operating efficiency (C), non-photochemical quenching (D) and fraction of PSII centres that are open (E). The error bar represents the standard error and n = 4.

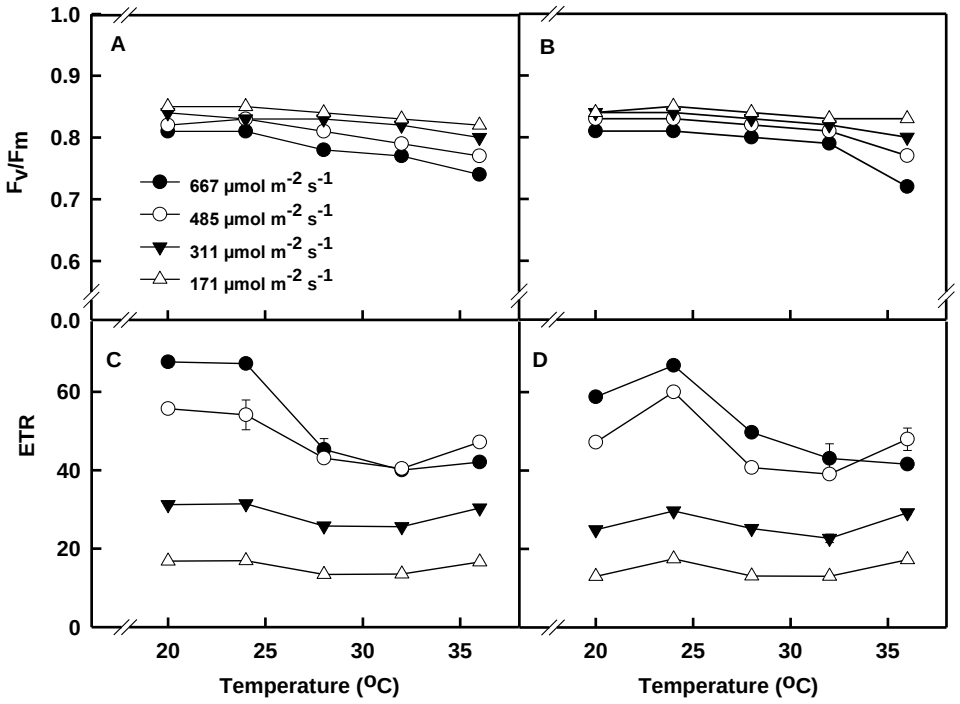
A
B
C
D
F_v/F_m
ETR
667 µmol m^{-2} s^{-1}
485 µmol m^{-2} s^{-1}
311 µmol m^{-2} s^{-1}
171 µmol m^{-2} s^{-1}
Temperature (^{O}C)
Temperature (^{O}C)

Fig. 1

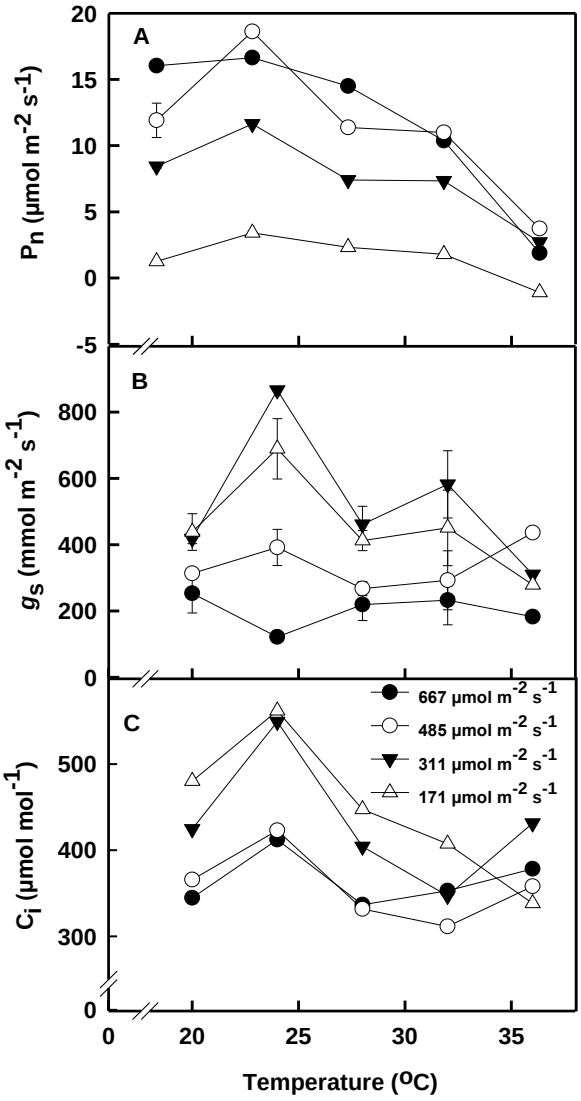
A
B
C
P_n (μmol m^{-2} s^{-1})
g_s (mmol m^{-2} s^{-1})
C_i (μmol mol^{-1})
667 μmol m^{-2} s^{-1}
485 μmol m^{-2} s^{-1}
311 μmol m^{-2} s^{-1}
171 μmol m^{-2} s^{-1}
Temperature (^{O}C)

Fig. 2

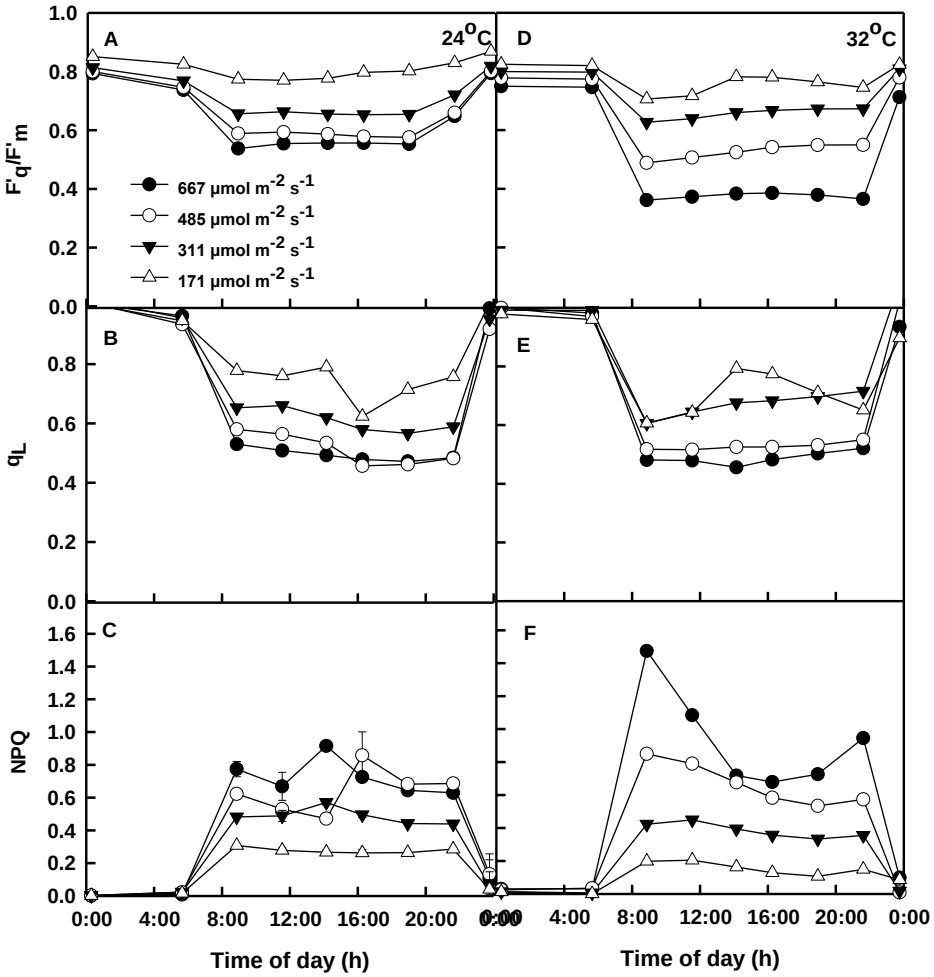
A
24°C
D
32°C
B
E
C
F
F'q/F'm
qL
NPQ
667 µmol m-2 s-1
485 µmol m-2 s-1
311 µmol m-2 s-1
171 µmol m-2 s-1
0:00
4:00
8:00
12:00
16:00
20:00
Time of day (h)

Fig. 3

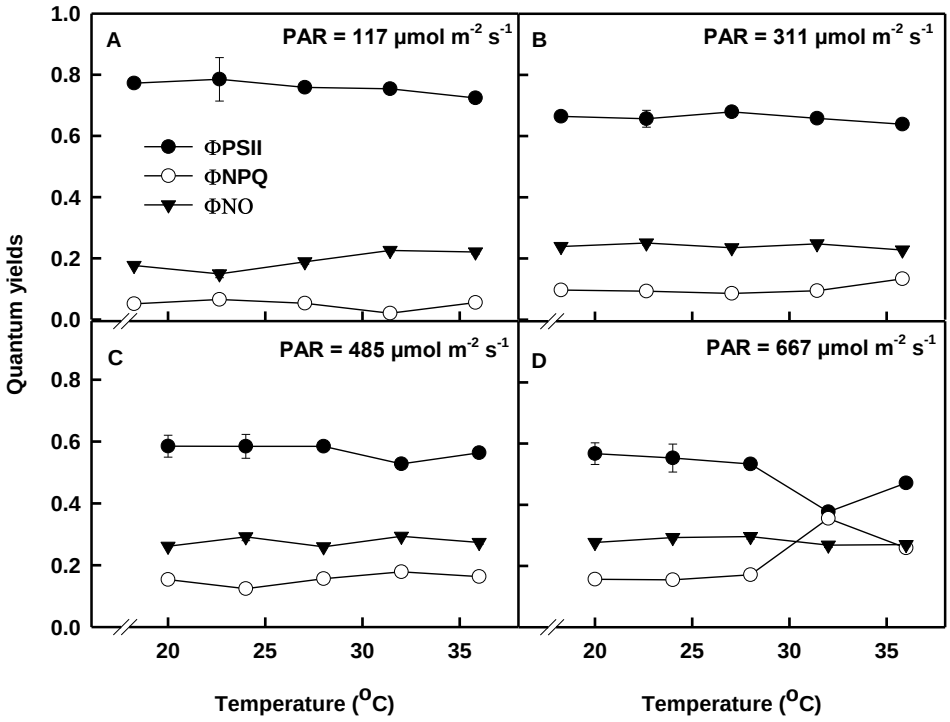
A
PAR = 117 µmol m-2 s-1
B
PAR = 311 µmol m-2 s-1
C
PAR = 485 µmol m-2 s-1
D
PAR = 667 µmol m-2 s-1
ΦPSII
ΦNPQ
ΦNO
Quantum yields
Temperature (OC)
Temperature (OC)

Fig. 4

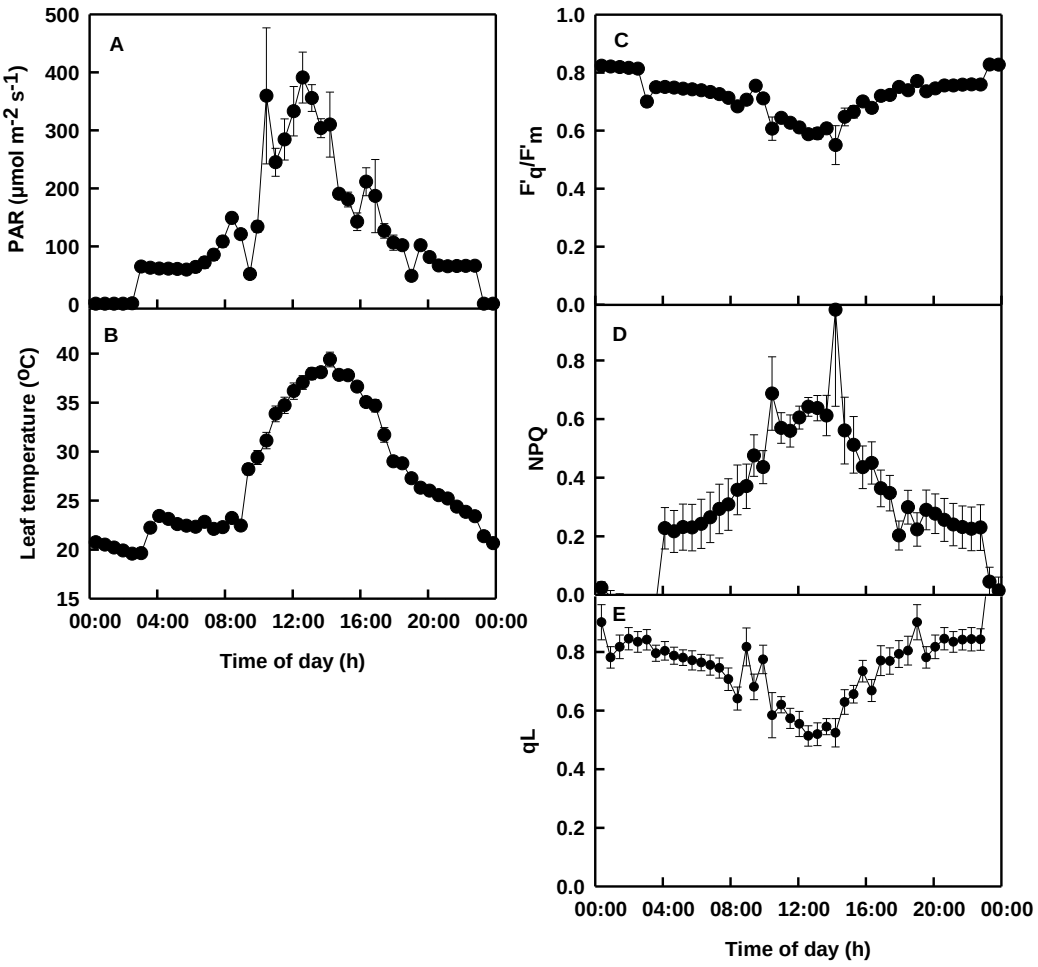
A
B
C
D
E
PAR (µmol m-2 s-1)
Leaf temperature (ºC)
F'q/F'm
NPQ
qL
Time of day (h)
Time of day (h)
00:00
04:00
08:00
12:00
16:00
20:00
00:00

Fig. 5